Dalton Transactions

ROYAL SOCIETY OF CHEMISTRY

PAPER

View Article Online
View Journal | View Issue

Cite this: *Dalton Trans.*, 2025, **54**, 15461

Inkless rewritable paper enabled by a scalable photochromic membrane

Junchao Liu, *[a] Chenfang Zhang,[a] Tianyu Huang,[a] Xusheng Guo,*[b] Zhenxin Kuang,[b] Rongwei Kou,[a] Zhong Yu,[a] Pan Jia[c] and Jingxia Wang *[b,d]

Received 17th August 2025,
Accepted 11th September 2025

DOI: 10.1039/d5dt01957e

rsc.li/dalton

Rewritable paper has attracted wide research attention in the field of environment-friendly information transmission owing to its potential to promote sustainable society development. Traditional organic dye-based rewritable paper may cause emission of pollution. To solve this problem, this study presents a flexible inorganic photochromic membrane by *in situ* growth of highly dispersed Cu-doped WO_3 nanoparticles in a polymethyl methacrylate matrix. Obvious discoloration of the as-prepared membrane can be repeated more than 200 times under alternating UV irradiation/heating based on an oxidation–reduction process between W^{6+} and W^{5+}. The proof of concept for rewritable paper and encryption algorithm is demonstrated herein. The results of this study are of great significance for the design and fabrication of a novel type of rewritable colorful paper.

Introduction

Papermaking is one of China's Four Great Inventions. It has had a profound impact on the development of the world's paper industry and the spread of human civilization. The global consumption of paper continues to grow to 300 million tons per year.[1] Global environmental issues of soil erosion, sandstorms and the greenhouse effect have been triggered owing to massive deforestation for papermaking. To solve those problems, rewritable paper based on organic dyes has been proposed by scientists.[2–7] The working principle of this type of paper is the controllable color change of the pigment, which may cause the emission of pollution.[1] Therefore, it is urgent to develop novel types of rewritable paper to solve the above problems.

Different from the traditional color display by chemical pigments, the discoloration of inorganic materials has become another coloration approach.[8–11] Typically, tungsten trioxide (WO_3) has attracted much research attention based on its high contrast ratios, excellent reversibility, lack of pollution and fast response to light.[12,13] The photochromic (PC) mechanism of WO_3 is that electrons transition from the valence band to the conduction band and form W^{5+} under UV irradiation.[14,15] Then it will gradually return to its original color after UV irradiation is stopped. However, most WO_3-based PC devices need liquid electrolytes containing redox media and the fabrication of free-standing, high strength and flexible WO_3-based membranes is difficult.[16,17] These phenomena limit its application in the field of rewritable paper. An effective approach to fabricate WO_3-based membranes is encapsulating WO_3 with a polymer binder.[18] However, fabricating such composite membranes with high transparency and uniformity still remains a challenge.

Writing information on paper is usually done with ink. In previous research on rewritable paper, water has been considered a superior ink due to its accessibility and non-polluting properties.[19–21] However, the resolution of the pattern usually is low due to the inevitable diffusion and evaporation of ink. Therefore, developing a new writing method is crucial for the field of rewritable paper. Among various stimuli, light is one of the most powerful and versatile physical stimuli based on its advantages of fast response, remote control, precise positioning and adjustable wavelength.[22–29] As a result, photo writing inkless rewritable paper has potential application value. In previous literature, Wang *et al.* fabricated a flexible inorganic PC membrane by *in situ* growth of highly dispersed Cu-doped WO_3 nanoparticles in a polymethyl methacrylate (PMMA) matrix and studied its application in the field of smart windows.[30] In the field of materials science, the development of new materials is crucial. At the same time, expanding the multi-domain applications of the same material is increasingly attracting the attention of scientists. In this paper, we

[a]*School of Sciences, Xi'an University of Technology, Xi'an 710048, China. E-mail: liujunchao17@mails.ucas.edu.cn*
[b]*Laboratory of Bio-inspired Smart Interface Science, Technique Institute of Physics and Chemistry, Chinese Academy of Sciences, Beijing 100190, China. E-mail: guoxusheng15@mails.ucas.ac.cn, jingxiawang@mail.ipc.ac.cn*
[c]*Hebei Key Laboratory of Inorganic Nanomaterials, College of Chemistry and Material Science, Hebei Normal University, Shijiazhuang 050024, China*
[d]*School of Future Technologies, University of Chinese Academy of Sciences, Beijing 101407, China*

conducted a detailed study on the application of the above-prepared membrane in the field of rewritable paper. For example, using a UV point light source instead of sunlight to trigger the tinting process. At the same time, using heating to accelerate the bleaching process. The as-prepared membrane demonstrates obvious and reversible color change under UV irradiation or heating based on an oxidation–reduction process between W^{6+} and W^{5+}. This process can be repeated more than 200 times. The pattern resolution of this system can reach 15 μm. The proof of concept for rewritable paper and encryption algorithm is demonstrated herein. The unique PC properties enable extensive applications in multi-functional optical devices, especially in the e-writing tablet field.

Experimental

Materials

1,2-Dichloroethane, copper(II) chloride and tungsten chloride were purchased from Aladdin. PMMA was purchased from Shanghai Macklin. DCM and DMF were purchased from Sinopharm Chemical. 30% Hydrogen peroxide was purchased from Xilong Scientific Co., Ltd.

Fabrication of Cu–W-PC membrane

60 μL 30% hydrogen peroxide, 0.015 g of copper(I) chloride and 0.3 g tungsten chloride were dissolved in 1.5 mL DMF and stirred for 2 h at room temperature. 4 g PMMA was dissolved in 50 mL DCM and stirred for 2 h at room temperature. The two solutions were mixed and stirred for 2 h to obtain a precursor solution for the membrane. The precursor solution was poured into an A4 size quartz tray and dried in an oven at 40 °C for 1 h. Finally, the Cu–W-PC membrane was obtained after demolding.

Fabrication of rewritable paper

A freshly made Cu–W-PC membrane was held horizontally. Then, the sample was irradiated by UV light (120 mW cm^{-2}, 4 s) in the presence of a mask to write a pattern. Finally, the pattern could be erased by heating (70 °C, 69 s).

Characterization

In this paper, optical images were obtained using an OLYMPUS BX53. SEM images were taken on a Thermo-4800 high-resolution field emission scanning electron microscope. The high-angle annular dark-field (HAADF) STEM images were obtained using a JEM-ARM300F. XPS measurements were accomplished *via* a photoelectron spectrometer (PHI5000 VersaprobeIII XPS) with an Al Kα radiation source. Atomic force microscopy (AFM) was undertaken on a Bruker Dimension Icon. Thermogravimetric analysis was carried out on a Q5000IR from 25 to 800 °C at a heating rate of 10 °C min^{-1} with N_2 as a protecting atmosphere. Transmittance spectra were obtained using a Cary 60 UV-vis spectrometer. UV light was obtained from the equipment of H086-425. X-ray diffraction measurements were conducted on a Rigaku D/max-2500 X-ray diffractometer.

Results and discussion

Fabrication and characterization of Cu–W-PC membrane

A highly transparent Cu–W-PC membrane was fabricated by a method of *in situ* growth of WO_3 nanoparticles in a PMMA matrix (Fig. 1A). First, a solution of PMMA in dichloromethane (DCM) and a solution of tungsten chloride (WCl_6) and copper (I) chloride (CuCl) in *N*,*N*-dimethylformamide (DMF) were uniformly mixed, then the system was poured into a mold and dried to form a membrane. In this process, WCl_6 was hydrolyzed to form WO_3 nanoparticles in the presence of H_2O. The gradual formation of the PMMA membrane was achieved based on the different boiling points of the two solvents (DCM 40 °C and DMF 153 °C), insolubility of WCl_6 in DCM and the low solubility of PMMA in DMF. This phenomenon allowed DCM to be completely evaporated before the formation of WO_3 nanoparticles. As a result, the nucleation process could be adjusted by encapsulating the precursors of the nanoparticles (WCl_6/CuCl/DMF) in the PMMA matrix, which controlled the particle growth and prevented particle agglomeration. In detail, PMMA chains were discrete in the DCM solvent, then the spacing between PMMA chains decreased and the chains became entangled with the evaporation of DCM. The generation of nanoparticles was subjected to the spatial domain of the PMMA chains after the complete evaporation of DCM. A

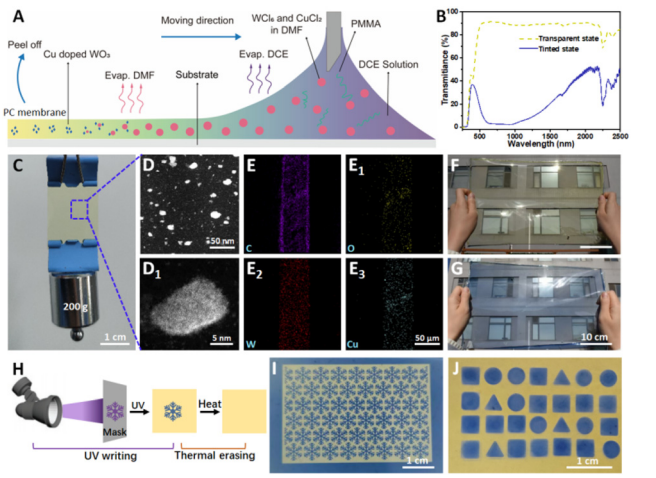

Fig. 1 Fabrication and corresponding working principle of the Cu–W-PC membrane. (A) Schematic illustration of the fabrication process for the Cu–W-PC membrane. The solutions of WCl_6/DMF and PMMA/DCM were uniformly mixed and dried in the mold. The PMMA and Cu-doped WO_3 gradually deposited in this process. (B) Transmittance spectra of the Cu–W-PC membrane in the transparent and tinted states. (C) Photo of membrane loaded with 200 g weight. (D and D_1) TEM images of WO_3 in the Cu–W-PC membrane. (E–E_3) SEM-EDS mapping of a cross section of the Cu–W-PC membrane. Photos of a 30 × 40 cm^2 Cu–W-PC membrane fabricated by the blade-coating method in the transparent state (F) and tinted state (G). (H) Schematic illustration of constructing a dynamic pattern on the Cu–W-PC membrane under UV irradiation/heating with the presence of a mask. Photo of (I) snowflake patterns or (J) different geometric patterns on the Cu–W-PC membrane.

rapid recovering bleaching process was achieved by introducing Cu ions into the PC membrane (Cu–W-PC membrane).[31,32] The as-prepared membrane showed a yellowish color after doping of Cu ions because of the formation of tetrachloro copper complex ion $[CuCl_4]^{2-}$. The Cu–W-PC membrane exhibited good mechanical properties and could support a weight of 200 g (Fig. 1C). The surface of the as-prepared membrane was smooth (Fig. S1 and S2). Fig. 1D, D_1 and S3 display the aberration-corrected high-angle annular dark-field scanning transmission electron microscopy (HAADF-STEM) images of WO_3 in the Cu–W-PC membrane. Abundant oxygen vacancies were observed in the surface of amorphous WO_3. The thickness of the as-prepared membrane was *ca.* 60 μm and a uniform distribution of nanoparticles throughout the thickness was observed (Fig. 1E–E_3 and S4). Besides, the as-prepared membrane had good thermal stability up to *ca.* 130 °C (Fig. S5). The Cu–W-PC membrane demonstrated a uniform coloration (tinted state) under sunlight irradiation and a recovery bleaching process (transparent state) under room light conditions. Fig. 1B presents transmittance spectra of the Cu–W-PC membrane in the different states. A high luminous transmittance of *ca.* 90% was observed in the transparent state, while the value decreased to *ca.* 20% in the tinted state. In particular, the Cu–W-PC membrane fabricated by the solution method was easily manufactured on a large scale. A scalable Cu–W-PC membrane was fabricated by the blade-coating method (Fig. 1F). And it also presented photochromism properties under sunlight (Fig. 1G). Inkless rewritable paper was constructed based on the photochromic properties of the Cu–W-PC membrane (Fig. 1H). Typically, the information was inputted under UV irradiation, then erased by heating. This process could be repeated at least 200 times. Complex snowflake patterns or different geometric patterns were easily achieved under UV irradiation with the presence of a mask (Fig. 1I and J).

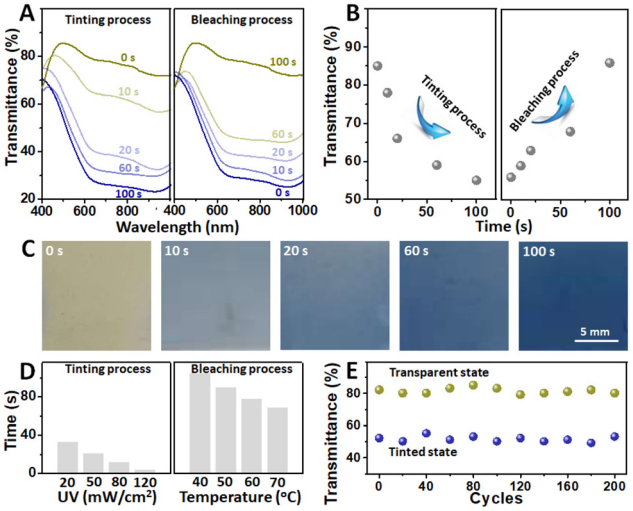

Fig. 2 Photochromic properties of the Cu–W-PC membrane. (A) Transmittance spectra of the Cu–W-PC membrane during the tinting (UV irradiation, 365 nm, 10 mW cm^{-2}) and bleaching processes (heating at 40 °C). (B) Transmittance change in the Cu–W-PC membrane at 500 nm during the tinting and bleaching processes. (C) Photos of the Cu–W-PC membrane during the tinting process (UV irradiation, 365 nm, 10 mW cm^{-2}). (D) Time required for complete tinting under different UV irradiation intensities (left) and complete bleaching at different heating temperatures (right). (E) Transmittance change in the Cu–W-PC membrane during 200 cycles of alternating tinting and bleaching processes.

Photochromic properties of the PC membrane

The photochromic properties of the Cu–W-PC membrane were further investigated by the change in transmittance under UV irradiation or heating (Fig. 2A and B). The transmittance of the membrane at 500 nm decreased from 85% to 78%, 66%, 59% and 55% with UV irradiation for 10 s, 20 s, 60 s and 100 s, respectively. Subsequently, the Cu–W-PC membrane recovered the transmittance to a large extent with 40 °C heating for 100 s. Fig. 2C shows photos of the Cu–W-PC membrane during the tinting process. The as-prepared membrane showed a yellowish color before UV irradiation, then gradually turned inky blue with 100 s UV irradiation. The time required for the tinting/bleaching process could be regulated by different intensities of the stimulus source (Fig. 2D). As the intensity of UV irradiation increased, the time required for the complete tinting process became shorter. Correspondingly, the bleaching process could be completed quickly as the temperature increased. Under optimal conditions, a 4 s tinting process and a 69 s bleaching process could be achieved. Under UV irradiation, the surface temperature of the Cu–W-PC membrane increased from 19.6 to 28.5 °C within 4 s, a moderate rise that avoided polymer degradation while slightly accelerating the coloration kinetics (Fig. S6). The tinting/bleaching process of the Cu–W-PC membrane demonstrated good cycling stability (Fig. 2E). The contrast between the transmittance at 500 nm of the Cu–W-PC membrane in the transparent and tinted states slightly decreased after 200 cycles.

Photochromic mechanism of the Cu–W-PC membrane

The photochromic mechanism of the Cu–W-PC membrane was further investigated in Fig. 3. As shown in Fig. 3A, the WO_3 nanoparticles absorb UV light and electron hole pairs are generated. W^{6+} is reduced to W^{5+} based on the process of photogenerated electrons trapped by oxygen vacancies on the surface of the WO_3 nanoparticles. The abundant oxygen vacancies on the surface result in an increased free charge density, and the free electrons oscillate under an external electromagnetic wave, giving rise to localized surface plasmon resonance. When Cu^{2+} is introduced into the membrane, some of the photogenerated electrons required for the tinting process are consumed by Cu^{2+}, reducing Cu^{2+} to Cu^{+}, which leads to a slower tinting process. The water molecules can capture photogenerated holes to form protons and oxygen. The charge of the captured photoelectrons can be balanced based on the insertion of protons into the tinted WO_3 nanoparticles.

Both W^{5+} and Cu^{+} are oxidized by oxygen in the air to form initially W^{6+} and Cu^{2+} under dark conditions. The bleaching

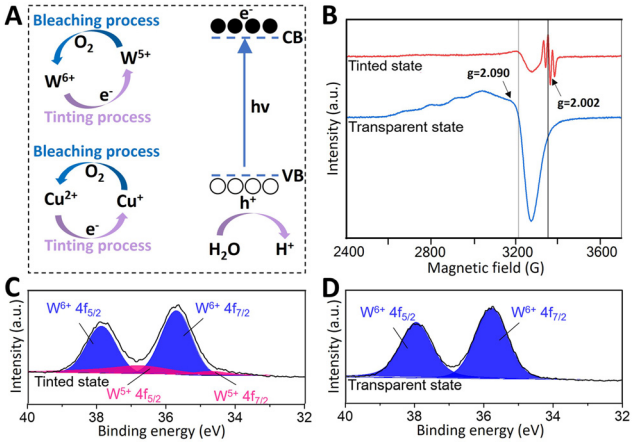

Fig. 3 Photochromic mechanism of the Cu–W-PC membrane. (A) Schematic illustration of the photochromic and bleaching mechanism of the Cu–W-PC membrane, including the generation of electron and hole pairs under light irradiation, the reduction of Cu^{2+} and W^{6+} by electrons, then oxidation by oxygen as the inverse process. (B) Electron paramagnetic resonance spectra of the Cu–W-PC membrane in the tinted state and transparent state. (C and D) XPS spectra of the Cu–W-PC membrane in the tinted state and transparent state for W 4f.

process of the W-PC membrane is slow because of the extremely tardy oxidation process of W^{5+}. In contrast, the unstable and easy to oxidize properties of Cu^{+} facilitate the bleaching process of the Cu–W-PC membrane based on the electron transfer from the occupied oxygen vacancies at the surface of the W^{5+} complex to the generated Cu^{2+} ions. In summary, a transfer process of electrons from W^{5+} to O_2 is achieved by the redox coupling of Cu^{2+}/Cu^{+}. The electron interactions between adjacent Cu^{2+}, Cu^{+}, W^{6+} and W^{5+} accelerate the bleaching process.

Electron paramagnetic resonance spectra of the Cu–W-PC membrane in the tinted state and transparent state are shown in Fig. 3B. In the tinted state, obvious peaks of oxygen vacancies at $g = 2.002$ were associated with W^{5+}. These changes were because of the reduction of W^{6+} to W^{5+} in WO_3 owing to the capture of photogenerated electrons by the oxygen vacancies during the tinting process. In addition, the strong signal of Cu^{2+} ($g = 2.090$) decreased significantly from the transparent state to the tinted state, which indicated the formation of Cu^{+}. X-ray photoelectron spectra (XPS) were recorded to verify the above proposed mechanism (Fig. 3C, D and Fig. S7). By comparing the XPS spectra of the Cu–W-PC membrane in the transparent and tinted states, peaks of W^{5+} were observed for the tinted state, which indicated that W^{6+} was partially reduced to W^{5+} by the photogenerated electrons.[33] Similarly, the change in the ratio of the peak area of Cu^{2+} and Cu^{+} proved the reduction process of Cu^{2+} to Cu^{+}.[34] The amorphous structure of WO_3 in the Cu–W-PC membrane was confirmed by X-ray diffraction (Fig. S8). A uniform distribution and adequate contact between W and Cu in the Cu–W-PC membrane were observed in the STEM-EDS mapping images (Fig. S3), which was conducive to the electron transfer.

Inkless rewritable Cu–W-PC paper

The photochromic properties of the Cu–W-PC membrane could be utilized to construct a dynamic pattern in the presence of a mask (Fig. S9). Resolution of the prepared pattern was investigated in Fig. 4A–C and S10. Different line widths were fabricated by adjusting the width of the mask, which could be applied to construct different patterns. The thinnest line width of 15 μm could be achieved under the optimized conditions (Fig. 4A). Then, different patterns of the skiing process were successively written on the same membrane after erasing the previous pattern (Fig. 4D–D_5), which indicated the realization of rewritable paper. First, a freshly-made Cu–W-PC membrane demonstrated a yellowish color (Fig. $4D_1$). Then, the membrane was irradiated by UV light in the presence of a mask. The area exposed to UV light quickly turned an inky blue color, which formed a skiing pattern (Fig. $4D_2$). The pattern could quickly disappear under 70 °C heating (Fig. $4D_3$). Different patterns were prepared sequentially on the same membrane by the above repeatable process (Fig. $4D_4$–D_5 and S11). In addition, more patterns could be sequentially written on the same membrane (Fig. 4E). Furthermore, programmatic writing/erasing of a pattern of letters (Fig. $4F_1$–F_4) was easily realized by defined region treatment, which contrib-

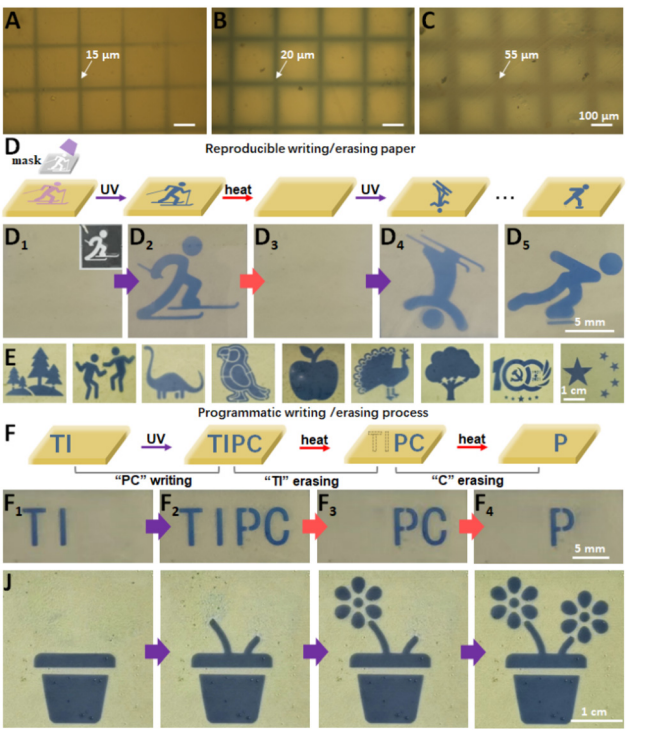

Fig. 4 Dynamic patterns on the Cu–W-PC membrane. (A–C) Different line widths under the different conditions. (D_1–D_5) Repeatable process of writing (UV irradiation, 120 mW cm^{-2}) and erasing (heating, 70 °C) of different patterns of the skiing process on the same membrane and corresponding schematic illustration (D). (E) The writing/erasing of more patterns on the same membrane. (F_1–F_4) Programmatic writing/erasing of a pattern of letters and (J) the process of gradually growing and blooming of a flower.

uted to the flexible input and delivery of sophisticated information. In detail, the letters "T", "I", "P", and "C" could be written or erased arbitrarily, such as stepwise writing "TIPC" (Fig. 4F_1 and F_2) or stepwise erasing "TIC" (Fig. 4F_3 and F_4). Similarly, the process of gradually growing and blooming of a flower was achieved in Fig. 4J.

The above pattern was inky blue in the pattern area, while the background area retained the original yellowish color of the membrane. Furthermore, an inverse mask (Fig. S12) was utilized to swap the colors of the two regions to construct an intricate pattern. Fig. 5A–F show some typical famous landmarks in China, which were made in the same membrane. For example, Great Wall (Fig. 5A), Temple of Heaven (Fig. 5B), Tian'anmen (Fig. 5C), Bird's Nest (Fig. 5D), Water Cube (Fig. 5E) and Oriental Pearl Tower (Fig. 5F). Practically, a complex pattern fabricated by light is preferable for realizing rewritable paper based on its high precision. The pattern on the membrane gradually appeared within 4 s of UV irradiation (Fig. S13). The as-prepared membrane demonstrated flexibility and transparency properties (Fig. 5G and S14). Finally, a large sized (*ca.* 20 × 25 cm^2) membrane with the handwritten letters "HELLO" was fabricated to satisfy the practical application needs (Fig. 5H). The Cu–W-PC membrane demonstrated excellent flexibility and was without fractures after 1000 bending cycles (Fig. 5I and J). Also, the transmission spectra of the as-prepared membrane remained almost the same after 1000 bending cycles (Fig. 5K). In addition, the as-prepared membrane showed good mechanical strength (tensile stress of 38.7 MPa), slightly lower than that of the PMMA membrane (Fig. 5L). The membrane showed a water contact angle of 71.3°, indicating moderate hydrophilicity due to the PMMA matrix and uniformly distributed Cu-doped WO_3 nanoparticles (Fig. S15). This multifunctional PC paper achieved by direct light acting on the membrane provides an insight for the fabrication of a novel optical device.

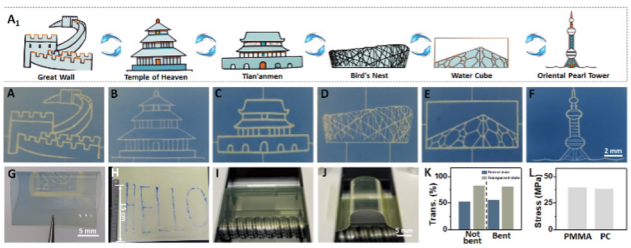

Fig. 5 Inkless rewritable PC paper. Complex patterns of famous landmarks in China and corresponding schematic illustration (A_1). (A) Great Wall, (B) Temple of Heaven, (C) Tian'anmen, (D) Bird's Nest, (E) Water Cube and (F) Oriental Pearl Tower. (G) Photo of as-prepared membrane. The membrane demonstrated flexibility. (H) A large sized (*ca.* 20 × 25 cm^2) paper with handwritten letters. (I and J) Photos of the Cu–W-PC membrane stretched and bent for 1000 cycles. (K) Transmittance of the Cu–W-PC membrane at 500 nm in the tinted state and transparent state before and after 1000 bending cycles. (L) Strain–stress values of PMMA and the Cu–W-PC membrane.

Encryption algorithm for a coding technique

To further expand the application scenarios of the as-prepared membrane, as a proof-of-concept, different pattern sequences can be additionally encrypted using a specific algorithm.[35,36] Morse code, invented in 1837, is an intermittent signal code that expresses different English letters, numbers, and punctuation marks through different permutations, which was originally used for telegraph communication and played an important role in early radio communication. Inspired by the rules of Morse code, a new type of encryption algorithm was developed (Fig. 6A). A restricted customized encryption algorithm will certainly be necessary for practical use rather than the known encryption algorithm. In this case, circle and square patterns were selected to encrypt the information units of alphabets and numbers, while a triangle shape was selected as a letter space, and double triangle patterns meant the end of the message. The complete encryption process is simply described as follows: first, the sender encrypted the initial message by sequentially writing patterns on the membrane according to a predetermined encryption algorithm. Then the receiver decrypted the cipher text into plain text according to the shared encryption algorithm and then obtained the secret message (Fig. 6B, "XUT 1919" meant Xi'an University of Technology was established in 1919). In addition, the information printed in the membrane could totally disappear within 12 hours, which improved the encryption and secure transmission of the information (Fig. 6C). This result provides a practical application of the photochromic membrane for a coding technique.

Conclusions

A rewritable writing/erasing paper can be achieved using a Cu–W-PC membrane based on the switchable structure color of the sample induced by the oxidation–reduction process between W^{6+} and W^{5+}. This rewritable PC paper demonstrates excellent performance with a quick response, flexible properties, and bright color printability to fully satisfy the requirements of daily use. Additionally, this PC paper presents outstanding repeatability for over 200 cycles with little decay. An encryption algorithm for a coding technique can be achieved

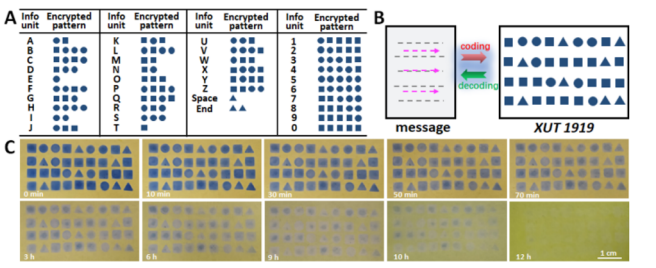

Fig. 6 PC membrane for a coding technique based on algorithm cryptography. (A) Shared encryption algorithm based on the modified Morse code. (B) The message made of different patterns based on the shared encryption algorithm. "XUT 1919" meant Xi'an University of Technology was established in 1919. (C) Photos of the membrane with the encrypted message taken at different times.

based on Morse code. All of these properties are helpful for the extensive application in a multi-functional optical display device, such as an e-writing tablet.

Author contributions

All authors have given approval to the final version of the manuscript.

Conflicts of interest

There are no conflicts to declare.

Data availability

The data supporting this article have been included as part of the supplementary information (SI). Supplementary information: SEM, AFM, and STEM–EDS images of surface and elemental distributions (Fig. S1–S3); cross-sectional morphology and elemental mapping (Fig. S4); thermal analysis (Fig. S5); surface temperature profiles under UV irradiation (Fig. S6); XPS and XRD characterizations (Fig. S7 and S8); optical images of micropatterns generated with different masks and irradiation times (Fig. S9 and S10, S12 and S13); reversible writing/erasing demonstrations (Fig. S11); transparency evaluation (Fig. S14); and water contact angle measurements (Fig. S15). See DOI: **https://doi.org/10.1039/d5dt01957e**.

Acknowledgements

The authors acknowledge the financial support from the Shaanxi Academy of Basic Sciences Fund (23JHQ079), Research Funding for Xi'an University of Technology (109-451023008), and NSFC (No. 22305063, 52373001, 51873221, 52073292, 51673207, 51373183 and 21988102).

References

1 M. Khazi, W. Jeong and J. Kim, Functional Materials and Systems for Rewritable Paper, *Adv. Mater.*, 2018, **30**, 1705310.
2 M. Belikov, A. Milovidova and M. Levlev, Novel Hydrochromic Dye of Butadienetricarbonitrile Series for Rewritable Self-Erasing Paper, *Dyes Pigm.*, 2024, **229**, 112298.
3 S. Huang, S. X.-A. Zhang, X. Qian, Y. Ni, Z. He, L. Sheng and J. Shen, Rice-Leaf-Mimetic Cellulosic Paper as a Substrate for Rewritable Devices and Biolubricant-Infused "Slippery" Surfaces, *Chem. Eng. J.*, 2024, **486**, 150073.
4 Y. Guan, X. Liu, S. Zhang and L. Sheng, Black Hydrochromic Fluoran Molecular Switches: Substituent Positional Isomerization Effects and Multicolor Water-Jet Printing, *J. Mater. Chem. C*, 2022, **10**, 15501.
5 W. Wang, N. Xie, L. He and Y. Yin, Photocatalytic Colour Switching of Redox Dyes for Ink-Free Light-Printable Rewritable Paper, *Nat. Commun.*, 2014, **5**, 5459.
6 M. Norouzi, Z. Mohamadnia, E. Ahmadi, N. Mahmoodi and H. Kiyani, Multicolor Switchable Latexes Containing a Bicyclic Aziridine Compound as Anticounterfeiting Inks for Reversible Photopatterning, *ACS Appl. Polym. Mater.*, 2024, **6**, 9784.
7 G. Xi, L. Sheng, J. Du, J. Zhang, M. Li, H. Wang, Y. Ma and S. Zhang, Water Assisted Biomimetic Synergistic Process and Its Application in Water-Jet Rewritable Paper, *Nat. Commun.*, 2018, **9**, 4819.
8 S. Liu, Y. Du, C. Tso, H. Lee, R. Cheng, S. Feng and K. Yu, Organic Hybrid Perovskite ($MAPbI_{3-x}Cl_x$) for Thermochromic Smart Window with Strong Optical Regulation Ability, Low Transition Temperature, and Narrow Hysteresis Width, *Adv. Funct. Mater.*, 2021, **31**, 2010426.
9 S. Liu, Y. Li, Y. Wang, K. Yu, B. Huang and C. Tso, Near-Infrared-Activated Thermochromic Perovskite Smart Windows, *Adv. Sci.*, 2022, **9**, 2106090.
10 X. Li, C. Cao, C. Liu, W. He, K. Wu, Y. Wang, B. Xu, Z. Tian, E. Song, J. Cui, G. Huang, C. Zheng, Z. Di, X. Cao and Y. Mei, Self-Rolling of Vanadium Dioxide Nanomembranes for Enhanced Multi-Level Solar Modulation, *Nat. Commun.*, 2022, **13**, 7819.
11 S. Wang, T. Jiang, Y. Meng, R. Yang, G. Tan and Y. Long, Scalable Thermochromic Smart Windows with Passive Radiative Cooling Regulation, *Science*, 2021, **374**, 1501.
12 J. Wang, Z. Wang, L. Cui, M. Zhang, X. Huo and M. Guo, Visible-Near Infrared Independent Modulation of Hexagonal WO_3 Induced by Ionic Insertion Sequence and Cavity Characteristics, *Adv. Mater.*, 2024, **36**, 2406939.
13 N. Li, Y. Zheng, L. Wei, H. Teng and J. Zhou, Metal Nanoparticles Supported on WO_3 Nanosheets for Highly Selective Hydrogenolysis of Cellulose to Ethylene Glycol, *Green Chem.*, 2017, **19**, 682.
14 A. Cohen, P. Mohapatra, S. Hettler, A. Patsha, K. Narayanachari, P. Shekhter, J. Cavin, J. Rondinelli, M. Bedzyk, O. Dieguez, R. Arenal and A. Ismach, Tungsten Oxide Mediated Quasi-van der Waals Epitaxy of WS_2 on Sapphire, *ACS Nano*, 2023, **17**, 5399.
15 J. Lochala, T. Taverne, B. Wu, M. Benamara, M. Cai, X. Xiao and J. Xiao, Tuning Solid Electrolyte Interphase Layer Properties through the Integration of Conversion Reaction, *ACS Appl. Mater. Interfaces*, 2019, **11**, 44204.
16 T. Dao, S. Park, S. Sarwar, H. Tran, S. Lee, H. Park, S. Song, H. Nguyen, K. Lee, C. Han and S. Hong, Novel Flexible Photochromic Device with Unprecedented Fast-Bleaching Kinetic Via Platinum Decoration on WO_3 Layer, *Sol. Energy Mater. Sol. Cells*, 2021, **231**, 111316.
17 S. Chun, S. Park, S. Lee, H. Nguyen, K. Lee, S. Hong, C. Han, M. Cho, H. Choi and K. Kwak, Operando Raman and UV-Vis Spectroscopic Investigation of the Coloring and

Bleaching Mechanism of Self-Powered Photochromic Devices for Smart Windows, *Nano Energy*, 2021, **82**, 105721.
18 Y. Zhou, N. Li, Y. Xin, X. Cao, S. Ji and P. Jin, Cs_xWO_3 Nanoparticle-Based Organic Polymer Transparent Foils: Low Haze, High Near Infrared-Shielding Ability and Excellent Photochromic Stability, *J. Mater. Chem. C*, 2017, **5**, 6251.
19 H. Liu, H. Ru, M. Sun, Z. Wang and S. Zang, Organic–Inorganic Manganese Bromide Hybrids with Water-Triggered Luminescence for Rewritable Paper, *Adv. Opt. Mater.*, 2021, **10**, 2101700.
20 C. Sun, H. Lu, C. Yue, H. Fei, S. Wu, S. Wang and X. Lei, Multiple Light Source-Excited Organic Manganese Halides for Water-Jet Rewritable Luminescent Paper and Anti-Counterfeiting, *ACS Appl. Mater. Interfaces*, 2022, **14**, 56176.
21 Y. Wei, Y. Chen, L. Hu, Y. Gao, H. Cai, C. Wu and Y. Yang, Unveiling the Potential of Highly Porous Covalent Organic Frameworks for Water-Jet Rewritable Papers, *ACS Appl. Mater. Interfaces*, 2024, **16**, 22248.
22 J. Liu, Y. Wang, J. Wang, G. Zhou, T. Ikeda and L. Jiang, Inkless Rewritable Photonic Crystals Paper Enabled by a Light-Driven Azobenzene Mesogen Switch, *ACS Appl. Mater. Interfaces*, 2021, **13**, 12383.
23 J. Liu, Y. Shang, J. Liu, J. Wang, T. Ikeda and L. Jiang, Janus Photochemical/Photothermal Azobenzene Inverse Opal Actuator with Shape Self-Recovery toward Sophisticated Motion, *ACS Appl. Mater. Interfaces*, 2022, **14**, 1727.
24 J. Liu, J. Wang, T. Ikeda and L. Jiang, Liquid-Phase Super Photoactuator through the Synergetic Effects of a Janus Structure and Solvent/Thermal/Photo Responses, *Adv. Funct. Mater.*, 2021, **31**, 2105728.
25 Y. He, H. Wang, C. He, R. Zeng, F. Cheng, Y. Hao, S. Chen and P. Zhang, A Porphyrin-Based Colorimetric and near Infrared Fluorescent Probe for Reversible and Rapid Detection of Diethyl Chlorophosphate, *Sens. Actuators, B*, 2025, **425**, 136983.
26 H. Liu, P. Zhang, C. Zhang, J. Chen and J. H. Jiang, Self-Assembly of a Dual-Targeting and Self-Calibrating Ratiometric Polymer Nanoprobe for Accurate Hypochlorous Acid Imaging, *ACS Appl. Mater. Interfaces*, 2020, **12**, 45822.
27 Y. Tian, Z. Zhou, J. Gong, J. Li, C. He, J. Chen, S. Chen, R. Zeng, Z. Mao and P. Zhang, Dual-Locking Fluorescent Nanoprobes for HAase-Triggered Carbon Monoxide Imaging in Living Cells, *Sens. Actuators, B*, 2023, **394**, 134421.
28 P. Zhang, X. Nie, M. Gao, F. Zeng, A. Qin, S. Wu and B. Tang, A Highly Selective Fluorescent Nanoprobe Based on AIE and ESIPT for Imaging Hydrogen Sulfide in Live Cells and Zebrafish, *Mater. Chem. Front.*, 2017, **1**, 838.
29 R. Zou, Y. Yu, H. Pan, P. Zhang, F. Cheng, C. Zhang, S. Chen, J. Chen and R. Zeng, Cross-Linking Induced Emission of Polymer Micelles for High-Contrast Visualization Level 3 Details of Latent Fingerprints, *ACS Appl. Mater. Interfaces*, 2022, **14**, 16746.
30 W. Meng, A. Kragt, Y. Gao, E. Brembilla, X. Hu, J. van der Burgt, A. Schenning, T. Klein, G. Zhou, E. van den Ham, L. Tan, L. Li, J. Wang and L. Jiang, Scalable Photochromic Film for Solar Heat and Daylight Management, *Adv. Mater.*, 2024, **36**, 2304910.
31 X. Dong, Z. Wu, Y. Guo, Y. Tong, X. Liu, L. Zhang and Y. Lu, Rational Modification in the Photochromic and Self-Bleaching Performance of Hierarchical Microsphere Cu@*h*-WO_3/WO_3·*n*H_2O Composites, *Sol. Energy Mater. Sol. Cells*, 2021, **219**, 110784.
32 T. Ma, B. Li, S. Tian, J. Qian, L. Zhou, Q. Liu, B. Liu, X. Zhao and G. Sankar, Reversible Photochromic $W_{18}O_{49}$: Mechanism Revealing and Performance Improvement for Smart Windows, *Chem. Eng. J.*, 2023, **468**, 143587.
33 X. Cao, Z. Chen, R. Lin, W. Cheong, S. Liu, J. Zhang, Q. Peng, C. Chen, T. Han, X. Tong, Y. Wang, R. Shen, W. Zhu, D. Wang and Y. Li, A Photochromic Composite with Enhanced Carrier Separation for the Photocatalytic Activation of Benzylic C–H Bonds in Toluene, *Nat. Catal.*, 2018, **1**, 704.
34 Y. Zhang, J. Zhao, H. Wang, B. Xiao, W. Zhang, X. Zhao, T. Lv, M. Thangamuthu, J. Zhang, Y. Guo, J. Ma, L. Lin, J. Tang, R. Huang and Q. Liu, Single-Atom Cu Anchored Catalysts for Photocatalytic Renewable H_2 Production with a Quantum Efficiency of 56%, *Nat. Commun.*, 2022, **13**, 58.
35 G. Rani, S. Ghoreishian, R. Umapathi, V. Vivekananthan and Y. Huh, A Biocompatible Triboelectric Nanogenerator-Based Edible Electronic Skin for Morse Code Transmitters and Smart Healthcare Applications, *Nano Energy*, 2024, **128**, 109899.
36 Y. Li, X. Zhou, Q. Yang, Y. Li, W. Li, H. Li, S. Chen, M. Li and Y. Song, Patterned Photonic Crystals for Hiding Information, *J. Mater. Chem. C*, 2017, **5**, 4621.